PAPER

Check for updates

Fitting ambiguities mask deficiencies of the Debye–Hückel theory: revealing inconsistencies of the Poisson–Boltzmann framework and permittivity†

Benjamin Janotta, [iD] *[a] Maximilian Schalenbach, [iD] *[a] Hermann Tempel [iD] [a] and Rüdiger-A. Eichel [iD] [abc]

The more than 100-year-old Debye–Hückel theory displays the most widely used approach for modeling ionic activities in electrolytes. The Debye–Hückel theory finds widespread application, such as in equations of state and Onsager's theory for conductivities. Here, a theoretical inconsistency of the Debye–Hückel theory is discussed, which originates from the employed Poisson–Boltzmann framework that violates the statistical independence of states presumed for the Boltzmann statistics. Furthermore, the static permittivity of electrolytic solutions is discussed as not directly measurable, while common methods for its extraction from experimental data are assessed as erroneous. A sensitivity analysis of modeled activity coefficients with respect to the permittivity and ionic radii as input parameters is conducted, showing that their influences overshadow physicochemical differences of common variations of Debye–Hückel models. Eventually, this study points out that the justification of the traditional and still often used Debye–Hückel models by experimental validation is affected by fitting ambiguities that eventually impede its predictive capabilities.

1 Introduction

In ideal solutions, colligative properties like the boiling-point elevation, freezing-point depression, and lowering of the vapour pressure are proportional to the concentration of the solute. The activity coefficient quantifies the deviations between real and ideal solutions by relating the real properties of solutes to their theoretical ideal values.[1] Debye and Hückel developed the first widely accepted model for the activity coefficient of dissolved ions, assuming electrostatic interactions between ions distributed in a dielectric continuum, with their distribution governed by the Poisson–Boltzmann (PB) equation.[2] In the Debye–Hückel (DH) theory, the ionic radii serve as input parameters to model the activity coefficient, while the impact of concentration dependence of the relative permittivity (also often referred to as dielectric constant) is still being investigated.[3] The modeled activity coefficients can be accurately matched to those measured of strong electrolytes

(completely or almost completely dissociated ions) at low concentrations using ionic radii as fitting parameters and a constant permittivity.[2] This agreement of model and experiment reasoned the success of the original DH theory and its rise to a standard model.[4] The DH theory displays the foundation for many electrolyte models, such as thermodynamic equations of state[5,6] and the conductivity.[7] However, the validity of the DH theory is restricted to low-molar electrolytes with monovalent ions.[8–11] This restricted validity is often ascribed to the linearization of the PB equation, the mean-field character of the electrostatic potential, and neglected physicochemical effects.

Although Arrhenius addressed the role of association in his 1903 Nobel Prize lecture, moderating his award-winning theory of electrolytic dissociation,[12,13] ion pairing was largely overlooked in the formulation of the DH theory in 1923 and in numerous subsequent extensions of the theory.[14] To extend the good match between the DH theory and experimental data to higher salt concentrations and to include physicochemical effects that are not incorporated in the original DH theory, a variety of extensions were proposed that can be categorized into:

(1) (Semi-) empirical models with parametrized concentration-dependent terms (like Hückel's model for the concentration-dependence of the permittivity,[15] and the Davies equation[16,17]).

(2) Virial expansions of the thermodynamic potentials (like Mayer's and Pitzers models[18–21]), which enable a

[a] *Fundamental Electrochemistry (IET-1), Institute of Energy Technologies, Forschungszentrum Jülich, Wilhelm-Johnen-Straße, 52425 Jülich, Germany.*
  E-mail: b.janotta@fz-juelich.de, m.schalenbach@fz-juelich.de
[b] *Institute of Physical Chemistry, RWTH Aachen University, 52062 Aachen, Germany*
[c] *Faculty of Mechanical Engineering, RWTH Aachen University, Aachen, Germany*
† Electronic supplementary information (ESI) available. See DOI: https://doi.org/10.1039/d5cp00646e

This journal is © the Owner Societies 2025

Phys. Chem. Chem. Phys., 2025, **27**, 7703–7715 | 7703

parameterization of interactions between electrolyte components using virial coefficients.

(3) Models for physicochemical effects of ions in solution (such as ion–solvent interaction,[14,22,23] short-range repulsion,[24] association[25]) that affect the thermodynamic potentials of the ions.

All these extensions come at the cost of an increased amount of parameters, as the parameters of one electrolyte are usually not transferable to other electrolytes or mixtures.[14] Although models of the third category aim to overcome the restricted applicability of parameters, the accuracy and validity of the used physicochemical models are debated[11,26–29] because isolating individual contributions to the activity coefficient from a single measurement technique is not possible.

The mean ionic activity coefficient of all ions in solution can be measured accurately by physicochemical properties such as electrochemical potentials, freezing point depression, and vapor pressure.[30] To better understand the individual contributions of the physiochemical effects (third category), other (macroscopic) properties such as the conductivity or vibrational spectra are often investigated.[31] The inferred contributions (such as the fraction of associated ions) are obtained by comparing the measurement with models for the measured property. A drawback of using models like Onsager's conductivity models[7] is their foundation in the DH theory or comparable theories for the ion distribution around a central ion and their dependence on several parameters.

In the DH theory, the ion radii and the electrostatic interactions between the ions determine the ion distribution around the central ion. Three DH models with different assumptions regarding the parameterization of the distance of closest approach (the sum of ionic radii a_i) between ions and the central ion are commonly used in the literature: (i) the full DH model (denoted as "DHFULL"), which accounts for different radii of the ions; (ii) the extended DH model (introduced by Hückel[15] and denoted as "EDH"), where a mean distance of closest approach for all ions is assumed; and (iii) the DH limiting law (denoted as "DHLL") for low concentrations, where the effects of the finite ion radius approach zero and are thus neglected. Repulsive interactions between ions around the central ion due to the finite volume (hard sphere) of the ions and the concentration dependence of parameters like the permittivity are not considered in the derivation of DH theory.

These shortcomings are reasons for the ongoing discussion on the validity and applicability of the DH models.[32–46] Consequently, adaptations[42,47–50] of and alternatives[51–53] to the DH theory were developed aiming to overcome these intrinsic shortcomings. Refined derivations of the DH theory starting with the PB equation such as the one by Shilov et al.[54,55] and Valiskó et al.[22,56] enable incorporating measurement data of the concentration dependent permittivity and predicting the activity coefficients over a larger range of concentrations without the introduction of new parameters. The non-monotonic behaviour of ionic activity coefficients of ions is explained by ion–solvent interaction. Alternative theories like the hypernetted chain theory,[51] and the Mean Spherical

Approximation (MSA)[52] intrinsically account for hard-sphere repulsion (and association), showing significant theoretical improvements compared to the DH theory. Unlike the explanation of Hückel[15] and Shilov et al.,[54,55] the non-monotonic increase of the activity coefficient is (largely) attributed to hard-sphere repulsion. By developing a modified PB theory based on thermodynamic perturbation theory, Budkov et al.[57,58] developed a model that intrinsically accounts for the local permittivity of the solvent and explicitly accounts for the dipole moment of the solvent and ions. Nevertheless, to date, theoretical models and foundations for electrolytes still lack a wide range of applicability, and improvements in electrolyte theories are regarded as the most crucial research area for applied thermodynamics.[59]

In this study, the assumptions underlying the derivation of the DH theory are examined and its parametrizability is critically investigated. First, the PB framework is discussed to violate the statistical independence of states presumed for the Boltzmann theory. Then, the measurement and calculation of the permittivity and its concentration dependence are critically discussed, showcasing the uncertainty of a property that is usually assumed to be known exactly. To assess the impact of parameter uncertainties, a sensitivity analysis is conducted comparing the three DH models with the MSA. Furthermore, contributions due to hard sphere repulsion of the ions, hydration, and association are compared which are used as physicochemical model extensions. The activity coefficient is calculated using the four named model contributions on presumed parameter intervals to mimic a predictive input of uncertain physical parameters. Additionally, the impact of the parameterization on the calculated conductivity is discussed, as transport properties are often used to determine thermodynamic properties like the degree of association. The uncertainty of the input parameters is shown to significantly impact the model results. Consequently, the good agreement between measurement data and models based on the DH theory are found to be a result of overfitting rather than a rigorous physicochemical modeling. With this approach, a critical discussion on the parameterization and physicochemical assumptions of the DH theory is presented, motivating the further development of modern models for electrolytic solutions as well as experimental techniques and atomistic modeling[60–64] for detailed validations.

2 Results and discussion

2.1 Conceptual inconsistencies of the Debye–Hückel theory

The qualitative and quantitative description of ion–ion and ion–solvent interactions for macroscopic models is intensely debated in the contemporary literature.[14,65] A key characteristic for models of (dilute) electrolytes is the propagation of the electrical field inside the electrolyte for which the Debye–Hückel (DH) theory displays the most widely used theory regarding macroscopic modeling.[4] In the following, the suitability of the DH theory as foundation for predictive electrolyte theories (in contrast to merely fitting available data) is

7704 | *Phys. Chem. Chem. Phys.*, 2025, **27**, 7703–7715

This journal is © the Owner Societies 2025

PCCP

Paper

discussed. Detailed analyses of mathematical assumptions (like the linearization of the Poisson–Boltzmann equation) during the derivation and further discussions (charging process) that often take the Poisson–Boltzmann framework as starting point can be found in the literature.[4,8,50,66]

2.1.1 The Poisson–Boltzmann framework. The following argumentation shows that the DH theory violates a rigorous application of fundamental principles of statistical mechanics, even if the mean field assumption is assumed to be correct (which is briefly discussed afterwards). The approximate nature of the DH theory arises from the violation of statistical independence of the microstates in the Poisson–Boltzmann equation. For the argumentation regarding this criticism, important fundamentals of the Boltzmann distribution are briefly recapitulated, before the approximate nature of the employed Poisson–Boltzmann distribution is discussed.

The Boltzmann distribution is derived for the assumption that the probability p^s to observe a system in a microstate (namely that a well-defined subsystem has the energy w^s) is proportional to the number of possible states M for a system with total energy W: $p \propto M(W - w^s)$.[67,68] Here, M is a function of $(W - w^s)$. The probability p^s for the microstate is

$$p^s = \frac{1}{Z}\exp\left(-\frac{w^s}{k_B T}\right), \tag{1}$$

where Z defines the canonical partition function (sum over all microstates)

$$Z = \sum_s \exp\left(-\frac{w^s}{k_B T}\right). \tag{2}$$

To avoid the necessity to calculate all microstates, the DH theory compares the probabilities to find an ion k in the two specific states denoted with superscripts ∞ and s. The superscript s denotes the state of interest with a specified energy w_k^s of k near a central ion, and ∞ a well known (reference) state far away from the central ion. By dividing one probability by another, Z gets eliminated and their relation can be expressed as

$$\frac{p_k^s}{p_k^\infty} = \exp\left(\frac{w_k^\infty - w_k^s}{k_B T}\right). \tag{3}$$

The probability p_k^s manifests as the concentration c_k of the macroscopic system. Using the electrostatic potential energy $w_k = z_k e \Phi_k$, where Φ_k, and z_k are the potential acting on k and the valence of k, and assuming that the potential far away from the central ion is negligible ($\Phi_k^\infty = 0$) reveals the starting point of the derivation of the DH theory

$$\frac{c_k^s}{c_k^\infty} = \exp\left(\frac{-z_k e \Phi_k^s}{k_B T}\right). \tag{4}$$

Since eqn (4) describes the distribution of a species k around the central ion j based on the mean concentration of the solution c_k^∞ (assuming radial symmetry), it is often written as the radial distribution function $g_{kj}(d) = c_k^s(d)/c_k^\infty$. The potential at a distance d from the central ion is determined by the

Poisson equation

$$\nabla_d^2 \Phi(d) = -\frac{F}{\varepsilon}\sum_j z_j c_j(d), \tag{5}$$

using the valence of the central ion as boundary condition, where F denotes the Faraday constant and ε the permittivity of the solvent. The electrostatic potential field emerges as a function of the concentrations of all ions, importantly, including $c_k(d)$. Noting that the potential field depends on c_k gives

$$\frac{c_k^s}{c_k^\infty} = \exp\left(\frac{-z_k e \Phi(c_k^{s*})}{k_B T}\right), \tag{6}$$

where $s*$ denotes all the states in which the ion is closer to central ion than in s. Using the proportionality between probability and concentration, again, the probability p_k^s of a species k to occupy a state s in the DH theory is expressed by

$$p_k^s = \frac{1}{Z}\exp\left(-\frac{w_k^s(p_k^{s*})}{k_B T}\right). \tag{7}$$

Hence, the energy w_k^s and the associated probability p_k^s depend on the probability for other states. Therefore, the microstates are not independent and the proportionality between the probability and the number of possible state M is violated. This dependence violates the statistical independence of the microstates presumed for Boltzmann statistics.

Fig. 1 illustrates the dependence of the probability for a state on the probability for a different state. The propagation of the electrostatic potential in Fig. 1(B) is determined by the probabilities for the states (by means of the concentrations, eqn (5)) in Fig. 1(A). Therefore, the probability to find an ion at a distance d from a central ion is calculated based on the potential energy (by means of the potential field) of different states, which, however are not simultaneously occupied.

The critique on the intrinsic approximation of the employed Poisson–Boltzmann equation discussed in this work is in
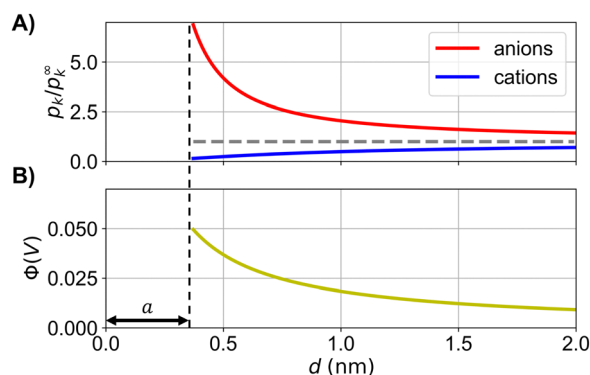

Fig. 1 (A) Calculated probability distributions of cations and anions, and (B) electrostatic potential around a central cation for a one-one electrolyte (solution of Debye and Hückel, see ESI† for equations), where a is the distance of closest approach. The probability for an ion to occupy a state in (A) affects the propagation of the electrostatic potential in (B) (see eqn (5)). Hence, the electrostatic potential energy of the same ion at a distance d is affected by the probability for the states with a smaller distance that d (which are not occupied at that time).

This journal is © the Owner Societies 2025

Phys. Chem. Chem. Phys., 2025, **27**, 7703–7715 | **7705**

contrast to statements in contemporary literature[4] claiming that the only approximation in the Poisson–Boltzmann equation is the used potential of mean force Φ (before linearization of the exponential). Importantly, even the DH limiting law is not free of the approximation discussed so far.

The approximate nature of the potential of mean force was criticised by Onsager who showed that eqn (4) is not self-consistent because the reciprocal relations (Onsager's Nobel prize in 1968) for two ions k and m are in general not fulfilled: $z_k e\Phi_m(d) \neq z_m e\Phi_k(d)$.[69] The inconsistency found by Onsager (and Fowler[70]) stems from the mean-field approximation, because the mean-field does not coincide with the potential of mean force (for the virtual displacement of the ion). The potential of mean force near a central ion calculated via the static Poisson–Boltzmann framework does not include the thermal ion movement by Brownian motion. Hence, the radial distribution function around the central ion derived in the static Poisson–Boltzmann framework does not portray the physical ion dynamics, leading to an intrinsic inaccuracy of the static fundament. In the presence of localized ions, the electrostatic potential field deviates significantly from the mean electrostatic potential field (DH theory) due to the de-localized (smeared) ion distribution. Furthermore, the average (mean) field due to localized ions does not coincide with the field due to smeared ions because of the non-linearity of the electric field strength as a function of the distance: $\Phi(\overline{c_i(d)}) \neq \overline{\Phi(c_i(d))}$. The bar over a variable denotes local averaging. Therefore, a localized ion at a distance d from a central ion is subjected to a different field and electrostatic potential energy than calculated in the DH theory. This argumentation coincides with the simulation results by Lyubartsev et al.[71] who used a reverse Monte Carlo approach for a NaCl solution. The Mean Spherical Approximation (MSA) is affected by similar mean-field assumptions, but the ion distribution is modeled based on a more realistic function for the potential of mean force.

2.1.2 The static permittivity. Fig. 2(A) shows measurement data of the static relative permittivity for aqueous NaCl solutions from the literature,[72–74] obtained via dielectric spectroscopy at probing frequencies in the microwave range. For pure water, the measured static relative permittivity is approximately $\varepsilon_r = 78$ (at 25 °C), while it decreases towards higher concentrations. The results from molecular dynamics (MD) simulations by Kalcher[75] using SPC/E water show a similar trend to the measurement data but start with an offset of about $\Delta \varepsilon_r = -6$. The negative offset is due to a too small dipole moment, and the non-polarizability of the water model.[76] Fig. 2(B) shows a histogram of the static relative permittivity of pure water calculated with different MD models as reported by Kadaoluwa et al.[77] (water models that were optimized to match a value for the relative permittivity are not included). Values for the static relative permittivity range from 51 to 197, while 60% are between 60 and 100, showing that MD simulations are currently still subjected to uncertainties.

The permittivity ε is typically measured by dielectric spectroscopy, in which a sinusoidal perturbation is applied and the sinusoidal response in terms of phase angle and amplitude is measured (like in impedance spectroscopy). For the dielectric
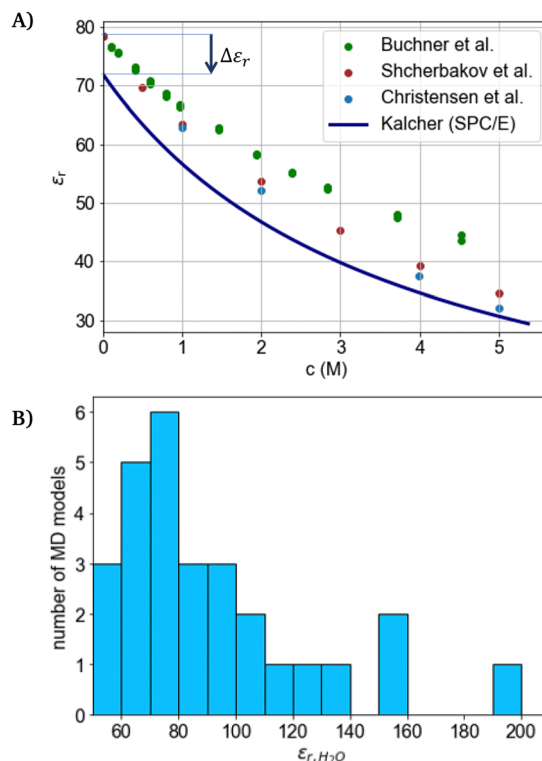

Fig. 2 (A) Measurement data and simulation results for aqueous NaCl solutions from literature.[72–75] (B) Simulation results from molecular dynamics simulations for water by Kadaoluwa et al.[77]

spectroscopy of aqueous solutions, microwave-frequencies between 10^8 and 10^{10} Hz are typically employed.[78] Lower frequencies increase the measurement challenges as the capacitive impedance diverges to infinity towards low frequencies. Hence, the permittivity obtained in the high-frequency regime are typically applied in the DH-theory, where they describe a static system without a perturbation (0 Hz). In the case of an ideal dielectric, which is purely capacitive and non-conducting, the permittivity is mostly frequency independent and can be extrapolated to that at zero frequency. Resonance phenoma in real dielectrics are described by the Debye relaxation model[79] in which the complex permittivity approaches a static value with decreasing frequency. Using the Debye model,[80,81] measurement data for water (a bad conductor) from measurement frequencies between 1 GHz and 40 GHz may be represented with an accuracy of 1% in this range.[82] However, for conducting electrolytes, the real and imaginary part of the permittivities typically diverge with power-law-dependencies towards low frequencies.[83,84] The power-law can be ascribed to the many-body interactions of strongly interacting bodies (such as water molecules), while weak interactions lead to the Debye characteristic.[84–87] Therefore, the static relative permittivity of water and especially electrolytes is not directly measurable and its estimation by fits[80] can be erroneous, while its real values might be significantly larger than the commonly measured values obtained at microwave-frequencies. Such larger values of the static permittivity of pure water were reported by some

7706 | *Phys. Chem. Chem. Phys.*, 2025, **27**, 7703–7715

This journal is © the Owner Societies 2025

authors based on molecular dynamics simulations (see Fig. 2(B)). Here, the static permittivity of a conducting medium is proposed to be undefined, as in electrostatics (at zero frequency) a conductor is electric field-free (Gauss law). Therefore, the permittivity of a conducting medium is only defined for the electrodynamic probing with alternating voltages. Thus, the static permittivity is considered inaccessible from measured data (also referring to the described diverging power-law-dependence towards zero frequency). Hence, the use of the static relative permittivity of conducting electrolytes displays a thus far unrecognized and unquantified source of error for the DH theory.

Additional arguments regarding the uncertainty of measured permittivities of electrolytes were discussed by Shilov *et al.*[54] (see their introduction), who incorporated the possibility to integrate an arbitrary function for the concentration dependent permittivity in the DH theory. Using concentration dependent literature data of the static relative permittivity (which are subjected to the discussed uncertainties), their model shows a qualitatively correct trend of the activity coefficients of solvent and solutes for one-one electrolytes.

The influence of the permittivity on the activity coefficient, especially the electrostatic contribution is still debated in the literature.[3,5,88–90] In the DH theory, the ions are assumed to be dispersed inside a dielectric continuum (primitive model), which allows for the derivation of analytical solutions of the models.[91] However, the permittivity is a heterogeneous property in electrolytes.[92] Molecular dynamics simulations support the conception of a heterogeneous permittivity as the dielectric response changes from bulk to confined fluids[93,94] and emphasize the anisotropy of the permittivity of water near charged surfaces.[95] Due to the preferred orientation of dipoles close to ions, the permittivity of the solvent close to the ion is smaller than that of the pure solvent which ultimately leads to the dielectric decrement for the bulk electrolyte.[46,92,96] The dielectric decrement affects the permittivity of the bulk electrolyte upon external excitation because less water molecules react to the excitation as depicted in Fig. 3. This explanation implies that the water molecules close to a central ion have more robust orientations to the ion than those of more distant ones. However, as long as the orientation of water molecules in the (first) hydration shell is not affected by the increased ion concentration, the electric field propagating from a central ion should also not be affected by the decrease of the

Fig. 3 Common explanation for the dielectric decrement: dipoles that are part of the hydration shell keep their orientation with respect to the ion upon external excitation.[46,92,96]

(dynamically measured) bulk permittivity. Therefore, the electrostatic contribution (DH theory) is affected differently by the dielectric decrement than the bulk electrolyte. In other words, the concentration dependence of the static permittivity measured for the bulk electrolyte (Fig. 2(A)) is probably not directly integrable for the electrostatic contribution (as exemplary done in Fig. 4(A), (C), and (D)).

2.1.3 Solvation shells. Solvation shells and the corresponding radii of hydrated ions in (aqueous) electrolytes are concentration dependent and intricately linked to the dielectric properties of the solvent. Molecular dynamics simulations show that the solvation shell is not rigid and that association may be favoured or not, depending on the valence and size of the considered ion and its counter ion.[99,100] The probability for association and the related disruption of the (first) solvation shell decreases towards larger ion radii of an ion, but increases with increasing radius of the counterion.[100]

The effect of ion solvation on the activity coefficient is often modeled using the Born term or derivations of it.[3] To evaluate the Born term, the dependence of the permittivity on the concentration is intrinsically required. Therefore, the uncertainty of the local dielectric properties also affects the Born term. The approach to calculate the contribution of the ion–solvent interaction using the Born term was criticized in general in a study by Simonin,[101] as the solution permittivity is probably irrelevant for the ion–solvent interaction it was meant to describe.

2.1.4 Dissociation, association, and homogeneous reactions. Measured association constants are often determined using indirect techniques such as conductivity or activity measurements, where the deviation of a model and the measurement data is attributed to association.[31] As a result, the accuracy of measured association constants depends not only on the precision of the measurements but also on the model used for data interpretation. For example, the DH theory (or Onsager's law for the conductivity) is often used to derive association constants,[102] so that the uncertainties and inaccuracies of the models discussed in this study affect the outcome of calculated association constants. The tendency of ions to associate depends on their valence, size, counterion, and the dielectric properties of the solvent. Associated ions decrease the effective ion concentration in the solution, thereby reducing the magnitude of the electrostatic contribution.[25,103] Furthermore, associated ions increase the bulk permittivity due to their strong dipole.[104] Ion pairs are typically differentiated between contact ion pairs, solvent shared ion pairs, and solvent separated ion pairs.[31] However, for modeling activity coefficients, dissociated and associated ions are usually distinguished based on the distance between an ion and the central ion, while their ratio is quantified by equilibrium constants (based on the mass action law).[31] Already in 1926, Bjerrum[25] pointed out that the choice of a specific cutoff distance for the definition of ion pairs is arbitrary. This cutoff distance is often defined as a minimum in a distribution function.[25,99] Models accounting for association usually include a parameter for the distance of closest approach. Hence, calculated equilibrium constants and fractions of free
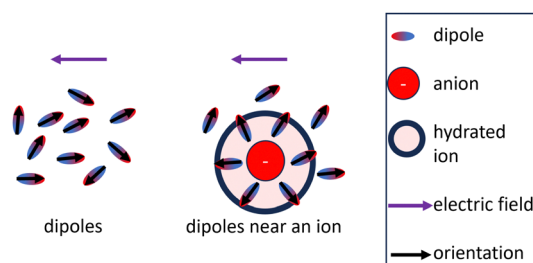
This journal is © the Owner Societies 2025

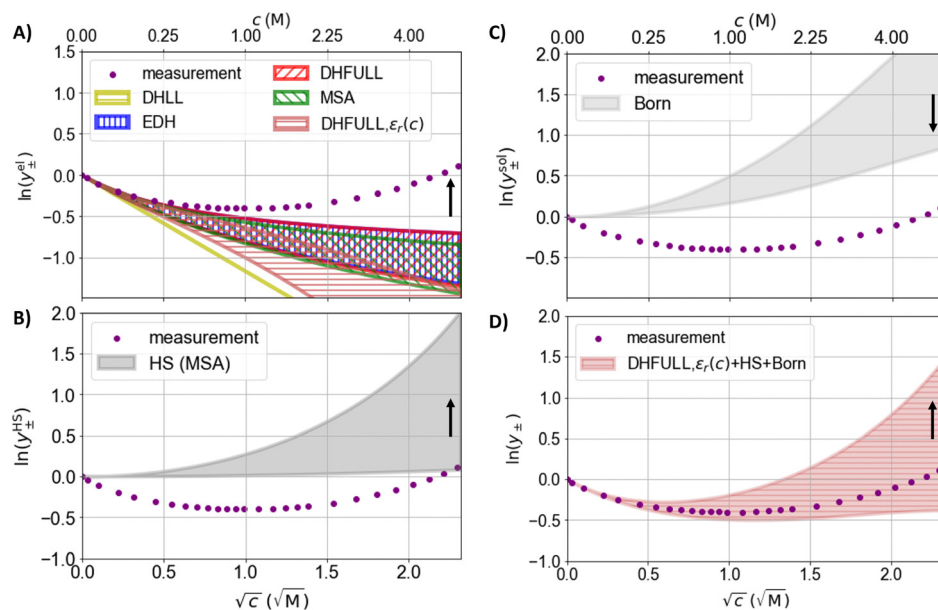*Phys. Chem. Chem. Phys.*, 2025, **27**, 7703–7715 | **7707**

Fig. 4 Logarithmic activity coefficient as a function of the square root of the concentration. Dots: measured activity coefficients for NaCl at 25 °C from the literature.[97,98] Coloured areas: activity coefficients between the lower and upper margins of the span of assumed ion radii calculated with different models. (A) The electrostatic contribution to the activity coefficient. (B) The hard sphere (HS) contribution to the activity coefficient. (C) The contribution due to Born hydration to the activity coefficient. (D) Sum of the logarithmic activity coefficients of the HS, Born hydration, and the electrostatic term of DHFULL including the concentration dependence of the permittivity. The black arrows indicate the direction the activity coefficients change towards larger ion radius/distance of closest approach.

ions depend on the chosen distance of closest approach and the cutoff distance. Consequently, verification of association models by comparison with experimental data is vital. The detailed overview over advantages and disadvantages of measurement techniques for ion pairing given in the comprehensive review on ion pairing by Marcus *et al.*[31] emphasizes the importance of spectroscopic, and relaxation methods.

2.2 Sensitivity analysis

In the following sensitivity analysis, the impact of the uncertain value of the (concentration dependent) permittivity is compared to the impact of the usual parameters, the ionic radii. The three DH models (DHLL, EDH, DHFULL) introduced in Sections 1 and 4.1.1 are applied to calculate activity coefficients and are (exemplary) compared to the MSA. Additionally, selected models for contributions that account for the hard sphere (HS) repulsion, ion hydration (Born term), and association are evaluated regarding their impact on the activity coefficient. For the variation of the distance of closest approach, intervals of 0.95 to 3.84 Å for Na^+ and 1.81 to 3.60 Å for Cl^- were chosen, corresponding to the Pauling radii and a hydration number of up to 7.9, and 6, respectively.[105] The static relative permittivity is varied between literature values of 78.14 and 95 as exemplary significantly higher value.

2.2.1 Models for the activity coefficient. Fig. 4 shows the measured activity coefficient of NaCl[97,98] at 25 °C and models for the electrostatic contribution to the activity coefficient calculated with the variation of the distance of closest approach. All depicted models for the electrostatic contribution show a good match with the experimental data at concentrations below 0.1 M. The Debye–

Hückel limiting law (DHLL) shows the highest negative deviation from the measurement data and is independent of the distance of closest approach. The extended Debye–Hückel model (EDH) and the full Debye–Hückel model (DHFULL) overlap almost perfectly for the considered radii due to the rather size-similar radii of the anion and cation considered in this work. The MSA shows a slightly more negative impact of the electrostatic contribution compared to EDH and DHFULL, but they still overlap to a large degree. This result coincides with the findings of Maribo-Mogensen *et al.*[106] who conclude that the MSA gives similar results as DHFULL if the distance of closest approach in the MSA is 5/6th that of DHFULL. Accounting for the concentration dependence of the static relative permittivity ($\varepsilon_r(c)$, eqn (18)) significantly increases the magnitude of the electrostatic contribution as shown for the DHFULL model. This result is qualitatively consistent with the (more rigorous) model of Shilov *et al.*[54] for the ion–ion interactions.

Fig. 4(B) shows the distribution of the hard sphere (HS) contribution for the given radius intervals. The HS contribution is more sensitive to the specified ion radii than the electrostatic contribution and is always positive. The spread of the HS contribution increases significantly with concentration. Fig. 4(C) shows the Born term accounting for the hydration of ions. Like the HS contribution, the activity coefficient calculated from the Born term is always positive, but the dependence on the ion radius is smaller. For the Born term, the same radii are assumed as for the other contributions (to reduce the degrees of freedom). Fig. 4(D) shows the summation of the three contributions in Fig. 4(A)–(C) combined using "DHFULL, $\varepsilon_r(c)$" from Fig. 4(A). For $c \leq 0.25$ M, the predicted activity

7708 | *Phys. Chem. Chem. Phys.*, 2025, **27**, 7703–7715

This journal is © the Owner Societies 2025

coefficient fits the measurement data well for the whole intervals of radii, while the spread around the measurement data is large for $c \geq 0.25$ M and increases.

Fig. 5 shows the measured activity coefficient of NaCl[97,98] at 25 °C and models for the electrostatic contribution to the activity coefficient calculated with the variation of the static permittivity. The magnitude of the electrostatic contributions (Fig. 5(A)) are inversely proportional to the static relative permittivity (the Pauling radii are used). The effect of the changed permittivity increases with increasing concentrations. Below $c = 0.04$ M, the static relative permittivity of 95 leads to a small positive deviation of the models from the measurement data. For higher concentrations, the prediction using $\varepsilon = 95$ is closer to the measurement data than 78.14. Fig. 5(B) shows the impact of assuming the static relative permittivity of water to be 95 on the Born term for concentrations up to the solubility limit (in contrast to Fig. 5(A)) assuming the same variation with concentration (eqn (18)). The absolute value of the activity coefficient decreases assuming a higher static relative permittivity for water and becomes significant above about 0.25 M.

To compare models for association, Fig. 6(A) shows the fraction of free ions α in a NaCl solution at 25 °C as a function of the concentration. In Bjerrum's model (based on the DH theory), the cutoff distance q between two ions for association for NaCl is smaller than the distance of closest approach of Na^+ and Cl^- necessary to fit measured activity coefficients (for all considered relative permittivities). Therefore, NaCl does not show association in this model and the fraction of free ions α

equals 1 for all concentrations.[25] Hence, NaCl is considered a strong electrolyte. The binding mean spherical approximation (BiMSA) predicts association even at low concentrations (≤ 0.25 M, Fig. 6(A)). The data of molecular dynamics (MD) using a SPC model in simulations for 1 m (molal) NaCl by Driesner et al.[99] indicate that incomplete dissociation needs to be considered even for a strong electrolyte like NaCl as only about 63% of the ions are completely dissociated. The simulation at 25 °C shows the formation of various aggregates besides the fully dissociated ions such as the species $NaCl_{(aq)}$, Na_2Cl^+, $NaCl_2^-$, and $Na_2Cl_{2(aq)}$. The resulting fraction of free ions is shown for all ions and only the fully dissociated Na^+ and Cl^-, respectively. Data from MD calculations by Alejandre et al.[107] using SPC/E, TIP4P/2005, and SPCE-FH force fields indicate negligable association for a concentration of 0.494 M, but a reduction of α to 0.55 at 2.375 M. Based on the concentrations given by Driesner et al.,[99] the fraction of free ions is calculated for all concentrations using the mass-action-law (MAL) assuming DHLL, and EDH-H for the activity coefficient, respectively. The MAL based on DHLL predicts increasing fractions of free ions above 1 M which is counterintuitive. Using the data of Driesner et al. as fix points for the mass action law leads to negligible dependence of α on the distance of closest approach (for EDH-H). Nevertheless, the data indicate the significance of ion association even for a strong electrolyte like NaCl in water, but also shows that the degree of association deviates strongly
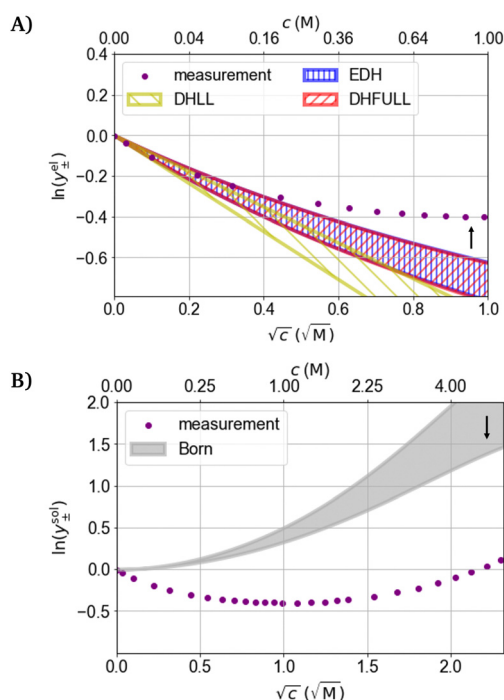
Fig. 5 Variation of the static relative permittivity of the solvent (from 78.14 to 95) in models for the activity coefficient (A) electrostatic contribution for DH models. (B) Born term. The arrows indicate the trend with increasing static relative permittivity of the solvent.
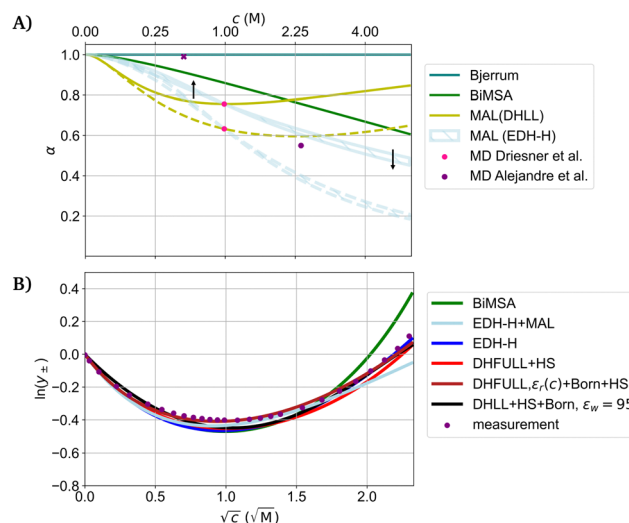
Fig. 6 (A) Fraction of free ions of NaCl at 25 °C as a function of the concentration for different models. The Bjerrum length at 25 °C in water for a 1-1 electrolyte is 3.55 Å which is smaller than the distance of closest approach for the radii considered in the fits in (B). Data by Alejandre et al.[107] using SPC/E, TIP4P/2005, and SPCE-FH force fields with similar results, the x denotes little association (without a given value). MD: molecular dynamics; BiMSA: binding means spherical approximation; MAL: mass action law (based on the MD by Driesner et al.[99] (pink points)). (B) Models with different physical interpretation fitted to measured activity coefficients of NaCl at 25 °C. The parameterization is summarized in the ESI.† EDH-H: DH theory as extended by Hückel; DHFULL: full DH theory; HS: hard sphere contribution; Born: Born term. BiMSA and EDH-H + MAL (upper limit of a) depict the same models in (A) and (B), respectively.

Table 1 Equilibrium constants K with units $[M]^{1-(m+n)}$ derived for the mass actions law (eqn (20))

$m + n$	2	3	4
DHLL	$3.095 10^{-3}$	$1.878 10^{-6}$	$3.478 10^{-9}$
EDH-H	$0.968 10^{-3}$	$0.588 10^{-6}$	$0.340 10^{-9}$

between the models. The arbitrariness of the parameterizations is exemplified in Table 1, where the equilibrium constants based on DHLL and EDH-H deviate up to a factor of ten for the same reaction.

The outcome of the models for the individual contributions for electrostatic interaction, hard sphere repulsion, solvation, and association (Fig. 4, 5, and 6(A)) show a significant dependence on their parameterization and model assumptions. Combining different contributions with an appropriate parameterization allows to match all the different models with measurement data as exemplified in Fig. 6(B). The four selected contributions here are combined to six different models for the activity coefficient of NaCl. Hückel's extension of the DH theory (EDH-H) accounting for the semi-empirical concentration dependence of the permittivity (denoted by C) is parametrized with $C = 0.1$. In combination with the MAL to account for association (EDH-H + MAL) it is parameterized by $C = 0.2$. The activity coefficients shown in Fig. 6(B) using EDH-H + MAL and BiMSA correspond to the graphs in Fig. 6(A). The BiMSA includes contributions due to electrostatics, hard sphere repulsion and association. Lastly, a model using DHLL, the hard sphere contribution and the Born term is shown assuming $\varepsilon_w = 95$ (eqn (18)). All models shown above describe different physicochemical assumptions, but (unsurprisingly) match the measurement data reasonably.

Importantly, Fig. 4–6 show that variation of the parameterization of the permittivity (be it the static value or the concentration dependence) can be compensated by fitting the ionic radii. The ionic radii used for the models depicted in Fig. 6(B) span over the complete intervals given in the Introduction.

2.2.2 Parameterization of transport properties. Transport properties such as diffusion coefficients and conductivities are used to explore thermodynamic characteristics such as association constants.[31] Fig. 7 shows experimental data for the conductivity of NaCl along with calculated data based on the Debye–Hückel–Onsager limiting law (DHO-LL), which is applicable only at low concentrations (≤ 10 mM), as well as two more modern conductivity models, DHO[108] and DHO3.[109] While Fig. 7(A) shows the impact of varying the ion radii (with $\varepsilon_r = 78.14$), Fig. 7(B) shows the impact of the static relative permittivity (using Pauling radii). The comparison of Fig. 7(A) and (B) shows that the variation of the permittivity of water has a much smaller impact than the ionic radii for the assumed intervals. Additionally, using experimental data for the viscosity in the electrophoresis term improves the trend of the modeled conductivities significantly. DHO3 with experimental viscosities and the Pauling radii shows a good match to the measurement data. Assuming this parameterization is accurate would implicate that no association occurs for NaCl (assuming associated
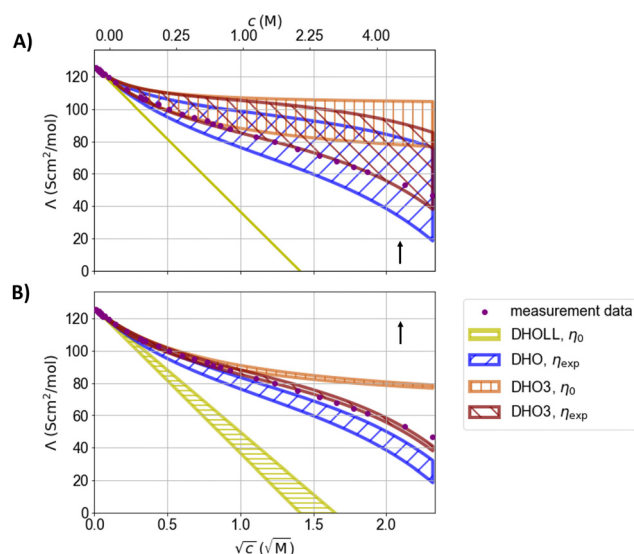

Fig. 7 Parameter variation of (A) the distance of closest approach from 2.76 to 7.44 Å (with $\varepsilon_r = 78.14$) and (B) the relative static permittivity of water from 78.14 to 95 (using Pauling radii) for conductivity models. The arrows indicate the impact of increasing the respective varied values. DHO-LL: Debye–Hückel–Onsager limiting law. DHO denoting the extension of the DHOLL from ref. 108 and DHO3 from ref. 109.

ions do not contribute to the conductivity); however, no association contradicts the results of advanced models graphed in Fig. 6(A).

2.3 Interdependence of properties, measurements, and models

For the development of predictive electrolyte theories (especially with a focus on multi-ion models), the microscopic interactions in electrolytes must be described by precise physicochemical models.[110] As shown above, almost arbitrary model combinations can be used to precisely describe experimental data; however, it confines the model to the domain of the data used for fitting, making extrapolations beyond this range generally unreliable.[14] Hence, this interchangeability of the contributions including their physicochemical parameterization prohibits the assessment of the validity of individual contributions based on fitting accuracies.[65] Furthermore, a challenge for the development of models and their parameterization is the interdependence and interaction of physical contributions as exemplary illustrated in Fig. 8. With changing concentration, the effect of one contribution (like the association) on the other contribution changes. This interdependence is seldom displayed in the models. As stated by Onsager[111] in 1968 with reference to association parameterization: "in a complete theory this [arbitrary definition of associated ions] would not matter; what we remove from one page of the ledger would be entered elsewhere with the same effect." To develop validate such models, a variety of independent measurement data is essential. Besides thermodynamic properties and their thermodynamic entanglement (e.g. by the Gibbs–Duhem equation), data based on non-equilibrium thermodynamics and transport models can help to develop and validate models but require a rigorous foundation.
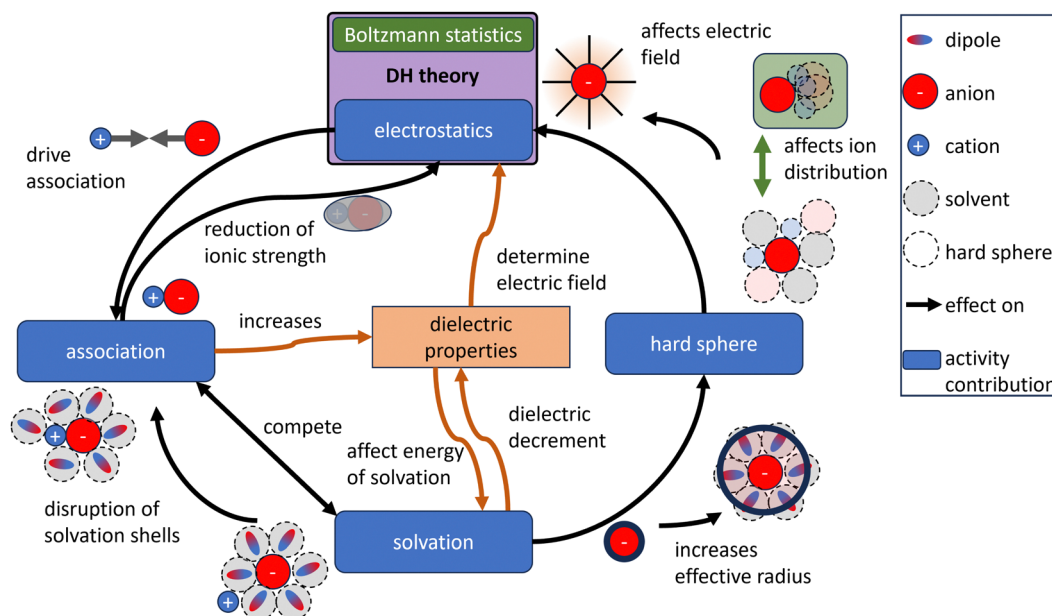
7710 | *Phys. Chem. Chem. Phys.*, 2025, **27**, 7703–7715

This journal is © the Owner Societies 2025

Fig. 8 Contributions to the activity (blue boxes) and their interdependences are exemplified for the electrostatic contribution, association, solvation, and the hard sphere contribution using simplified sketches. The Debye–Hückel (DH) theory does not incorporate any dependencies of other contributions.

The DH theory predicts the electrostatic contribution to the activity coefficient, while other contributions like association, hard sphere repulsion and hydration are neglected during its derivation. Although these contributions can be added explicitly to improve the alignment with measured electrolyte properties, the interdependence between the electrostatic contribution and these other contributions is not considered in the DH theory (see Fig. 8). Introducing for example the hard sphere contribution during the derivation of the electric field, changes it and the outcome of the activity coefficient (compare DH theory to MSA). It is also shown above that the parametrizability of the DH theory in combination with other contributions allows to model a wide range of possible trends for measurement data up to their solubility limit. However, if the electrostatic contribution is modeled incorrectly at moderate to high concentrations (as key assumptions are violated) while the measurement data is fitted well, then the other contributions are inevitably also modeled incorrectly. The uncertainty of the DH theory at moderate concentrations is transferred into other model contributions, while these contributions are being studied. Therefore, a good match between model and measurement does not necessitate a physically accurate model. Since modern theories aim to predict electrolyte properties based on detailed, quantitative physical understanding in contrast to just describing them, it is questionable whether the DH theory is the proper basis for such theories, especially since more physically detailed models exist. For now, the enduring success of the Debye–Hückel theory, spanning more than a century, is attributed in part to its high degree of parametrizability, rather than to its physical rigor.

3 Conclusions

This work has explored physicochemical assumptions, simplifications, and fitting ambiguities of the Debye–Hückel theory. In detail, the solution of the Poisson–Boltzmann equation as it is employed in the Debye–Hückel theory is shown to violate assumptions necessary for its derivation. Furthermore, the uncertainty of the static permittivity due to measurement challenges and its impact on exemplary model contributions are discussed. For that purpose, the influence of the uncertainty of the permittivity is compared to the parametrizability of the distance of closest approach (linked to the ionic radius) for the Debye–Hückel models, as well as the mean spherical approximation, hard sphere repulsion, Born term, and ion association. The analysis demonstrates that the ability of these models to fit experimental data does not necessitate an accurate physical representation of the system. In particular, uncertainties for the value and the concentration dependence of the permittivity can be compensated by the parameterization and model selection. Therefore, an assessment of any contribution and its parameterization without a fundamentally rigorous background is ambiguous. The interdependence of the DH theory and theories for other contributions is discussed, revealing that the complexity of physiochemical interactions in electrolytes cannot be easily displayed by non-interacting models.

4 Methods

The activity coefficient of a species describes the (energetic) deviation of a compound from ideal behavior in a mixture. The non-ideality of ions in solution consists of multiple dominant contributions. Here, the electrostatic (el) contribution, the hard sphere (HS) contribution, the solvation (sol) and the association (asso) are discussed. The activity coefficient y_i of ion i is related to the individual contribution[112] by eqn (8)

$$\ln(y_i) = \ln(y_i^{el}) + \ln(y_i^{HS}) + \ln(y_i^{sol}) + \ln(y_i^{asso}) + \ldots \quad (8)$$

The mean molar activity coefficient $y_\pm$ of a binary salt is defined as the average of the single ion activity coefficients[46] eqn (9)

$$y_\pm^{\nu_+ + \nu_-} = y_+^{\nu_+} y_-^{\nu_-}. \tag{9}$$

4.1 The electrostatic contribution

The first model for ions in solution to be successfully matched with experimental data (for activity coefficients, and for the conductivity) was the Debye–Hückel (DH) theory.[2,113] The primary distinction between electrolytes and non-electrolytes in terms of their contributions to the activity coefficient stems from the electrostatic interactions between ions. The DH theory aims to describe this contribution but is restricted to low concentrations.[8] In the literature, different equations for the DH theory (based on different simplifications) are used.[114] The three most important ones,[114] namely the Debye–Hückel limiting law (DHLL), the extended Debye–Hückel theory (EDH) and the full Debye–Hückel theory (DHFULL) are briefly discussed in the following.

4.1.1 The Debye–Hückel theory. The complete activity coefficient $y_{i,\text{DHFULL}}^{\text{el}}$ as predicted by Debye and Hückel reads[2]

$$RT \ln\left(y_{i,\text{DHFULL}}^{\text{el}}\right) = -\frac{F^2}{4\pi\varepsilon} \frac{\kappa z_i^2}{6 N_A} \left(2X_i + \frac{\sum\limits_k c_k z_k^2 \sigma'_k}{\sum\limits_k c_k z_k^2} \right), \tag{10}$$

where R denotes the ideal gas constant, T temperature, F Faraday's constant, z the valence, c concentration, ε the permittivity (with $\varepsilon = \varepsilon_0 \varepsilon_R$, ε_0 representing the vacuum permittivity and ε_R denoting the static relative permittivity), and N_A is Avogadro's number. The substituents X_k and σ'_k are defined by

$$X_i = \frac{3}{(\kappa a_k)^3} \left(\frac{3}{2} + \ln(1 + \kappa a_k) - 2(1 + \kappa a_k) + \frac{1}{2}(1 + \kappa a_k)^2 \right), \tag{11}$$

$$\sigma'_k = \frac{3}{(\kappa a_k)^3} \left(1 + (1 + \kappa a_k) - 2\ln(1 + \kappa a_k) + \frac{1}{2(1 + \kappa a_k)} \right), \tag{12}$$

with

$$\kappa^2 = \frac{F^2}{\varepsilon RT} \sum_k z_k^2 c_k, \tag{13}$$

and a_i representing the ionic radius. The characteristic Debye length λ is defined by $\lambda = \kappa^{-1}$.[2] For very dilute solutions, the effect of the ion radius approaches zero, leading to the Debye–Hückel limiting law (DHLL, eqn (7)):[2]

$$RT \ln\left(y_{i,\text{DHLL}}^{\text{el}}\right) = -\frac{F^2}{4\pi\varepsilon} \frac{\kappa z_i^2}{2 N_A}. \tag{14}$$

Hückel[15] assumed a common mean distance of closest approach a for both ions in binary electrolytes during the derivation of the influence of the permittivity. This model is called extended DH theory (EDH), leading to:

$$RT \ln\left(y_{i,\text{EDH}}^{\text{el}}\right) = -\frac{F^2}{4\pi\varepsilon} \frac{z_i^2}{2 N_A} \frac{\kappa}{1 + \kappa a}. \tag{15}$$

4.1.2 The Mean Spherical Approximation. In contrast to the DH theory, the Mean Spherical Approximation (MSA) treats ions as impenetrable spherical molecules.[10] This approach incorporates the finite size of ions and accounts for hard-sphere interactions between them, providing a more realistic representation of ion behaviour in solutions than the DH theory.[10] In contrast to the analytical DH models, this more complex framework requires numerical solutions. The electrostatic contribution $y_{i,\text{MSA}}^{\text{el}}$ is obtained by solving a system of equations that originates from the interdependence of the hard-sphere ion distribution and the electric field. The approach exemplary used within this work is discussed by Verweij et al.[115]

4.2 The hard sphere contribution

The hard sphere contribution y_i^{HS} accounts for the repulsive short-range interactions by treating ions as impenetrable spheres that cannot overlap.[10] The hard sphere contribution is assumed to account for the contribution to the free energy by volume exclusion due to the ions and the hydration shell.[116] The equations for the hard sphere contribution used in this work are available in the literature.[115]

4.3 Hydration and changing relative permittivity

Besides the volume exclusion, the solvation (hydration) of ions also affects the solution permittivity.[15] To account for the hydration, Hückel[15] extended the DH theory with the semi-empirical extension for the concentration dependence of the permittivity (EDH-H) using a constant parameter C. The activity coefficient of the EDH-H is calculated by:

$$RT \ln\left(y_k^{\text{EDH-H}}\right) = -\frac{F^2}{4\pi\varepsilon} \frac{z_k^2}{2 N_A} \frac{\kappa}{1 + \kappa a} + 2Cc. \tag{16}$$

If association is neglected, C is set to $C = 0.1$ here, while $C = 0.2$ is used in combination with models for association (for better fits). Another model accounting for the hydration by means of the changing permittivity is the Born term, which is a semi-empirical expression inspired by the model for the Gibbs solvation energy. Eqn (17) shows a simplified model for the Born term which is discussed in detail by Silva et al.[3] (being denoted as 'Born-0' there)

$$RT \ln\left(y_k^{\text{sol}}\right) = \frac{F^2 z_k^2}{8\pi\varepsilon_0 b_k N_A} \left(\frac{1}{\varepsilon_r} - \frac{1}{\varepsilon_w} \right), \tag{17}$$

where ε_w denotes the static relative permittivity of pure water, and b_k denotes the Born radius. In this study, we restrict the Born radius to coincide with the distance of closest approach ($b_k = a_k$) to reduce the degree of freedom for the parameterization (instead of calculating if from the Gibbs solvation energy or using it as fitting parameter). The concentration dependent permittivity of aqueous NaCl is modeled using the equation from Buchner et al.:[72]

7712 | *Phys. Chem. Chem. Phys.*, 2025, **27**, 7703–7715

This journal is © the Owner Societies 2025

$$\varepsilon_{\mathrm{r}}(c) = \varepsilon_{\mathrm{w}} - 15.2c + 3.64c^{3/2}. \qquad (18)$$

where $\varepsilon_{\mathrm{w}} = 78.14$ is the static relative permittivity of water.

4.4 Association

Association has a substantial impact on electrolyte properties as it decreases the fraction of free ions α (number of ions in solution divided by number of ions assuming complete dissociation) in solution, directly affecting other contributions such as the electric contribution, or properties like the conductivity.[31] Therefore, an accurate association model is vital for modeling electrolytes. Three models for the association are briefly compared within this study: the Bjerrum model,[25] a mass action law (MAL) based on results from molecular dynamics simulations,[99] and an association model based on MSA.[116] The first extension of the DH theory for association was proposed by Bjerrum.[25] Bjerrum defined ions as associated when their distance is smaller than a cutoff distance q where the probability of to find an ion near a central ion has a minimum:

$$q = \frac{e^2 z_{\mathrm{c}} z_k}{4\pi\varepsilon k_{\mathrm{B}} T} \qquad (19)$$

The association is described by the fraction of free ions α, which can be calculated based on the energy to separate the ions.[25] As a compensation for a lack of reliable measurement data, results from molecular dynamics simulations for a NaCl solution from Driesner *et al.*[99] are shown for comparison with the models. Based on these results, equilibrium constants are derived in this work to show results for a simplified mass action law,[117] assuming an equilibrium constant K for each associated species:

$$K_{n+m} = \frac{y[\mathrm{Na}_m\mathrm{Cl}_n^{m-n}]}{y^m[\mathrm{Na}^+]^m y^n[\mathrm{Cl}^-]^n}. \qquad (20)$$

The simulation data of Driesner *et al.*[99] shows that at 25 °C only $n,m \in [0,1,2]$ are relevant. Here, the activity coefficient of all anions and cations is assumed to equal the mean activity coefficient for this equation, whereas the activity coefficient of neutral species is assumed to equal 1.

The last association model is based on the Binding Mean Spherical Aapproximation (BiMSA) which extends the MSA to explicitly account for the equilibrium between free ions and ion pairs. Details on and the derivation of the BiMSA can be found in the literature.[103,116] For the simulation, the published code of Crothers *et al.*[116] was adapted for aqueous NaCl and used. In a 1-1 electrolyte, α can be calculated based on an equilibrium constant, the activity coefficient and geometrical data of the ions in solution.[116]

4.5 Conductivity models

Conductivity measurements are often used to investigate electrolyte properties such as the degree of association of the ions in solution.[109,118,119] In detail, the difference between model and measurement is typically explained with association.[31] Here, three different conductivity models are compared, starting with the most important one: the Debye–Hückel–Onsager

limiting law (DHOLL). The DHOLL reads[120]

$$\Lambda = \Lambda^0 - \kappa\left(\frac{|z_-z_+|e^2 q\Lambda^0}{3\varepsilon k_{\mathrm{B}}T(1+\sqrt{q})} + \frac{F^2(|z_+|+|z_-|)}{6\pi\eta N_{\mathrm{A}}}\right), \qquad (21)$$

where Λ denotes the molar conductivity, Λ^0 the limiting molar conductivity, I the ionic strength and $q = 0.5$ for 1-1 electrolytes. The first term inside the brackets describes the relaxation effect, while the second term describes the electrophoresis. The extension of the DHOLL for the finite size of ions by Robinson and Stokes[108] which introduces a factor of $1/(1 + \kappa a)$ as a factor for the bracket in eqn (21) is also implemented in this study. Furthermore, the model named 'DHO3 presented by Naseri Boroujeni *et al.*[121] is implemented here, representing an exemplary modern model that is based on the Debye–Hückel–Onsager theory but uses the crystallographic ion radii.

Author contributions

Benjamin Janotta: conceptualization, methodology, software, writing – original draft preparation, visualization. Dr Maximilian Schalenbach: conceptualization, methodology, writing – original draft preparation, visualization, funding acquisition, supervision. Dr Hermann Tempel: writing – reviewing and editing, project administration, funding acquisition. Prof. Dr Rüdiger-A. Eichel: project administration, funding acquisition.

Data availability

The data supporting this article have been included as part of the ESI.†

Conflicts of interest

There are no conflicts to declare.

Acknowledgements

Notes and references

1 J.-L. Burgot, *The Notion of Activity in Chemistry*, Springer International Publishing, Cham, 2016.
2 P. Debye and E. Hückel, *Phys. Z.*, 1923, **24**, 185–206.
3 G. M. Silva, X. Liang and G. M. Kontogeorgis, *Fluid Phase Equilib.*, 2023, **566**, 113671.
4 G. M. Kontogeorgis, B. Maribo-Mogensen and K. Thomsen, *Fluid Phase Equilib.*, 2018, **462**, 130–152.
5 L. Rueben, P. Rehner, J. Gross and A. Bardow, *J. Chem. Eng. Data*, 2024, **69**, 3044–3054.
6 B. Maribo-Mogensen, *Development of an electrolyte CPA equation of state for applications in the petroleum and chemical industries*, DTU Chemical Engineering,

This journal is © the Owner Societies 2025

Phys. Chem. Chem. Phys., 2025, **27**, 7703–7715 | 7713

Department of Chemical and Biochemical Engineering, Kgs. Lyngby, 2014.

7 L. Onsager and R. M. Fuoss, *J. Phys. Chem.*, 1932, **36**, 2689–2778.

8 J. S. Newman and N. P. Balsara, *Electrochemical systems*, John Wiley & Sons, Inc, Hoboken, 4th edn, 2021.

9 O. Redlich, *Chem. Rev.*, 1946, **39**, 333–356.

10 J.-P. Simonin and O. Bernard, *Fluid Phase Equilib.*, 2023, **571**, 113805.

11 E. A. Guggenheim, *London, Edinburgh Dublin Philos. Mag. J. Sci.*, 1935, **19**, 588–643.

12 S. Arrhenius, *Dissertation*, Academy of Sciences, Stockholm, 1884.

13 S. Arrhenius, *Z. Phys. Chem.*, 1887, **1U**, 631–648.

14 G. M. Kontogeorgis, A. Schlaikjer, M. D. Olsen, B. Maribo-Mogensen, K. Thomsen, N. von Solms and X. Liang, *Int. J. Thermophys.*, 2022, **43**, 1–68.

15 E. Hückel, *Phys. Z.*, 1925, **1925**, 93–147.

16 C. W. Davies, *J. Chem. Soc.*, 1938, 2093.

17 C. W. Davies and T. Shedlovsky, *J. Electrochem. Soc.*, 1964, **111**, 85C.

18 J. E. Mayer, *J. Chem. Phys.*, 1950, **18**, 1426–1436.

19 K. S. Pitzer, *Thermodynamics*, McGraw-Hill, New York, 3rd edn, 1995.

20 D. G. Archer, *J. Phys. Chem. Ref. Data*, 1991, **20**, 509–555.

21 F. Pérez-Villaseñor, G. A. Iglesias-Silva and K. R. Hall, *Ind. Eng. Chem. Res.*, 2002, **41**, 1031–1037.

22 J. Vincze, M. Valiskó and D. Boda, *J. Chem. Phys.*, 2010, **133**, 154507.

23 J.-P. Simonin, *J. Mol. Liq.*, 2023, **380**, 121713.

24 R. Triolo, J. R. Grigera and L. Blum, *J. Phys. Chem.*, 1976, **80**, 1858–1861.

25 N. Bjerrum, *K. Dan. Vidensk.*, 1926, **7**, 1.

26 L. Onsager, *Ann. N. Y. Acad. Sci.*, 1945, **46**, 241–265.

27 J. Prausnitz, R. Lichtenthaler and E. G. de Azevedo, *Molecular Thermodynamics of Fluid-Phase Equilibria*, Pearson Education, Limited, Hoboken, 3rd edn, 1998.

28 P. M. V. Résibois, *Electrolyte theory. An elementary introduction to a microscopic approach*, Harper & Row, New York, 1968, p. 29.

29 D. Fraenkel, *J. Phys. Chem. B*, 2011, **115**, 14634–14647.

30 G. N. Lewis and M. Randall, *J. Am. Chem. Soc.*, 1921, **43**, 1112–1154.

31 Y. Marcus and G. Hefter, *Chem. Rev.*, 2006, **106**, 4585–4621.

32 D. Fraenkel, *Mol. Phys.*, 2010, **108**, 1435–1466.

33 D. Fraenkel, *J. Comput. Chem.*, 2015, **36**, 2302–2316.

34 D. Fraenkel, *J. Chem. Theory Comput.*, 2018, **14**, 6434–6442.

35 D. Fraenkel, *J. Chem. Theory Comput.*, 2018, **14**, 2609–2620.

36 P. van der Weg, *Am. J. Anal. Chem.*, 2018, **09**, 406–422.

37 E. A. Guggenheim, *Trans. Faraday Soc.*, 1959, **55**, 1714.

38 E. A. Guggenheim, *Trans. Faraday Soc.*, 1960, **56**, 1152.

39 T. Biver and F. Malatesta, *J. Chem. Theory Comput.*, 2018, **14**, 6427–6433.

40 C. W. Outhwaite, M. Molero and L. B. Bhuiyan, *J. Chem. Soc., Faraday Trans.*, 1993, **89**, 1315–1320.

41 K. S. Pitzer, *J. Chem. Soc., Faraday Trans. 2*, 1972, **68**, 101.

42 J.-L. Liu and C.-L. Li, *AIP Adv.*, 2019, **9**, 1–6.

43 D. L. Bowers and E. E. Salpeter, *Phys. Rev.*, 1960, **119**, 1180–1186.

44 Z. Abbas, M. Gunnarsson, E. Ahlberg and S. Nordholm, *J. Phys. Chem. B*, 2002, **106**, 1403–1420.

45 T. S. Sørensen, *J. Chem. Soc., Faraday Trans.*, 1990, **86**, 1815–1843.

46 R. A. Robinson, *Electrolyte solutions: Robinson RA, Stokes RH (2002) Electrolyte solutions*, Dover, Mineola, 2002.

47 P. Vieillefosse, *J. Phys.*, 1981, **42**, 723–733.

48 T. Xiao and X. Song, *J. Chem. Phys.*, 2011, **135**, 104104.

49 M. Costa Reis, *ChemTexts*, 2021, **7**, 1–17.

50 P. B. van der Weg, *J. Colloid Interface Sci.*, 2009, **339**, 542–544.

51 J. Rasaiah, *Chem. Phys. Lett.*, 1970, **7**, 260–264.

52 L. Blum, *Mol. Phys.*, 1975, **30**, 1529–1535.

53 A. O. Quiñones, L. B. Bhuiyan and C. W. Outhwaite, *Condens. Matter Phys.*, 2018, **21**, 23802.

54 I. Y. Shilov and A. K. Lyashchenko, *J. Phys. Chem. B*, 2015, **119**, 10087–10095.

55 I. Y. Shilov and A. K. Lyashchenko, *J. Solution Chem.*, 2019, **48**, 234–247.

56 M. Valiskó and D. Boda, *J. Phys. Chem. B*, 2015, **119**, 14332–14336.

57 Y. A. Budkov, A. L. Kolesnikov and M. G. Kiselev, *EPL*, 2015, **111**, 28002.

58 Y. A. Budkov and A. L. Kolesnikov, *J. Stat. Mech.:Theory Exp.*, 2022, **2022**, 053205.

59 E. Hendriks, G. M. Kontogeorgis, R. Dohrn, J.-C. de Hemptinne, I. G. Economou, L. F. Žilnik and V. Vesovic, *Ind. Eng. Chem. Res.*, 2010, **49**, 11131–11141.

60 K. A. Maerzke, T. J. Yoon and R. P. Currier, *J. Chem. Eng. Data*, 2022, **67**, 3661–3671.

61 J.-C. Chen, B. Reischl, P. Spijker, N. Holmberg, K. Laasonen and A. S. Foster, *Phys. Chem. Chem. Phys.*, 2014, **16**, 22545–22554.

62 P. Habibi, P. Dey, T. J. H. Vlugt and O. A. Moultos, *J. Chem. Phys.*, 2024, **161**, 1–10.

63 L. C. Kröger, S. Müller, I. Smirnova and K. Leonhard, *J. Phys. Chem. A*, 2020, **124**, 4171–4181.

64 B. Svensson and B. Jönsson, *Chem. Phys. Lett.*, 1984, **108**, 580–584.

65 N. Novak, F. Yang, M. D. Olsen, X. Liang, N. von Solms, I. G. Economou, M. Castier, J.-C. de Hemptinne, A. Z. Panagiotopoulos and G. M. Kontogeorgis, *Fluid Phase Equilib.*, 2025, **594**, 114339.

66 J. G. Kirkwood and J. C. Poirier, *J. Phys. Chem.*, 1954, **58**, 591–596.

67 L. Boltzmann, 1877, pp. 373–435.

68 J. Williard Gibbs, *Elementary principles in statistical mechanics: developed with especial reference to the rational foundations of thermodynamics*, Charles Scribner's Sons, 1902.

69 L. Onsager, *Chem. Rev.*, 1933, **13**, 73–89.

70 R. H. Fowler, *Trans. Faraday Soc.*, 1927, **23**, 434.

71 A. P. Lyubartsev and A. Laaksonen, *Phys. Rev. E:Stat. Phys., Plasmas, Fluids, Relat. Interdiscip. Top.*, 1995, **52**, 3730–3737.

72 R. Buchner, G. T. Hefter and P. M. May, *J. Phys. Chem. A*, 1999, **103**, 1–9.

7714 | *Phys. Chem. Chem. Phys.*, 2025, **27**, 7703–7715

This journal is © the Owner Societies 2025

73 V. V. Shcherbakov, Y. M. Artemkina and E. N. Korotkova, *Russ. J. Inorg. Chem.*, 2014, **59**, 922–926.

74 J. H. Christensen, A. J. Smith, R. B. Reed and K. L. Elmore, *J. Chem. Eng. Data*, 1966, **11**, 60–63.

75 I. Kalcher, *Aqueous Electrolytes: Ion-Specific Structure and Thermodynamics (Dissertation)*, 2011.

76 R. D. Mountain and A. Wallqvist, *A collection of results for the SPCE water model*.

77 S. P. Kadaoluwa Pathirannahalage, N. Meftahi, A. Elbourne, A. C. G. Weiss, C. F. McConville, A. Padua, D. A. Winkler, M. Costa Gomes, T. L. Greaves, T. C. Le, Q. A. Besford and A. J. Christofferson, *J. Chem. Inf. Model.*, 2021, **61**, 4521–4536.

78 *Microwave and Radio-Frequency Technologies in Agriculture: An Introduction for Agriculturalists and Engineers*, ed. G. Brodie, M. V. Jacob and P. Farrell, De Gruyter, Warschau/Berlin, 2016.

79 P. Debye, *Polar molecules*, Dover Publications, INC, 1929, vol. 48.

80 R. Gulich, M. Köhler, P. Lunkenheimer and A. Loidl, *Radiat. Environ. Biophys.*, 2009, **48**, 107–114.

81 A. de Ninno, E. Nikollari, M. Missori and F. Frezza, *Phys. Lett. A*, 2020, **384**, 126865.

82 D. P. Fernández, Y. Mulev, A. R. H. Goodwin and J. M. H. L. Sengers, *J. Phys. Chem. Ref. Data*, 1995, **24**, 33–70.

83 A. K. Jonscher, *Nature*, 1977, **267**, 673–679.

84 A. K. Jonscher, *IEEE Trans. Electr. Insul.*, 1992, **27**, 407–423.

85 L. A. Dissado, *Phys. Scr.*, 1982, **T1**, 110–114.

86 L. A. Dissado and R. M. Hill, *Proc. R. Soc. London, Ser. A*, 1983, **390**, 131–180.

87 L. A. Dissado, *Chem. Phys.*, 1984, **91**, 183–199.

88 N. Yao, X. Chen, X. Shen, R. Zhang, Z.-H. Fu, X.-X. Ma, X.-Q. Zhang, B.-Q. Li and Q. Zhang, *Angew. Chem.*, 2021, **60**, 21473–21478.

89 Q. Lei, B. Peng, L. Sun, J. Luo, Y. Chen, G. M. Kontogeorgis and X. Liang, *AIChE J.*, 2020, **66**, 1–13.

90 C. Zhang, S. Yue, A. Z. Panagiotopoulos, M. L. Klein and X. Wu, *Phys. Rev. Lett.*, 2023, **131**, 076801.

91 D. Zuckerman, M. Fisher and B. Lee, *Phys. Rev. E:Stat. Phys., Plasmas, Fluids, Relat. Interdiscip. Top.*, 1997, **56**, 6569–6580.

92 N. Gavish and K. Promislow, *Phys. Rev. E*, 2016, **94**, 012611.

93 M. H. Motevaselian and N. R. Aluru, *ACS Nano*, 2020, **14**, 12761–12770.

94 Y. Mao, T. Zhou, L. Xu, W. Wu, R. Wang, Z. Xiong, D. Wu and H. Shi, *Chem. Eng. J.*, 2022, **435**, 134750.

95 A. Limaye, D. Suvlu and A. P. Willard, *Faraday Discuss.*, 2024, **249**, 267–288.

96 J. B. Hasted, D. M. Ritson and C. H. Collie, *J. Chem. Phys.*, 1948, **16**, 1–21.

97 R. A. Robinson, *Electrolyte Solutions*, Butterworths Scientific Publication, 1959.

98 T. W. Chapman and J. Newman, *A compilation of selected thermodynamic and transport properties of binary electrolytes in aqueous solution*, 1968.

99 T. Driesner, T. M. Seward and I. G. Tironi, *Geochim. Cosmochim. Acta*, 1998, **62**, 3095–3107.

100 P. Kumar, M. D. Bharadwaj and S. Yashonath, *RSC Adv.*, 2016, **6**, 114666–114675.

101 J.-P. Simonin, *J. Chem. Phys.*, 2019, **150**, 244503.

102 D. D. Perrin, *Ionisation constants of inorganic acids and bases in aqueous solution*, Pergamon Press, Oxford, 2nd edn, 1982, vol. 29.

103 H. Krienke, J. Barthel, M. Holovko, I. Protsykevich and Y. Kalyushnyi, *J. Mol. Liq.*, 2000, **87**, 191–216.

104 P. Wang and A. Anderko, *Fluid Phase Equilib.*, 2001, **186**, 103–122.

105 D. H. Powell, A. C. Barnes, J. E. Enderby, G. W. Neilson and P. S. Salmon, *Faraday Discuss. Chem. Soc.*, 1988, **85**, 137.

106 B. Maribo-Mogensen, G. M. Kontogeorgis and K. Thomsen, *Ind. Eng. Chem. Res.*, 2012, **51**, 5353–5363.

107 J. Alejandre, G. A. Chapela, F. Bresme and J.-P. Hansen, *J. Chem. Phys.*, 2009, **130**, 1–10.

108 R. A. Robinson and R. H. Stokes, *J. Am. Chem. Soc.*, 1954, **76**, 1991–1994.

109 S. Naseri Boroujeni, B. Maribo-Mogensen, X. Liang and G. M. Kontogeorgis, *J. Phys. Chem. B*, 2023, **127**, 9954–9975.

110 P. M. May and D. Rowland, *J. Chem. Eng. Data*, 2017, **62**, 2481–2495.

111 *The collected works of Lars Onsager: (with commentary)*, ed. L. Onsager and P. C. Hemmer, World Scientific, Singapore, Repr edn, 1998, vol. 17.

112 C. Held, L. F. Cameretti and G. Sadowski, *Fluid Phase Equilib.*, 2008, **270**, 87–96.

113 P. Debye and E. Hückel, *Phys. Z.*, 1923, **24**, 305.

114 G. M. Silva, X. Liang and G. M. Kontogeorgis, *Mol. Phys.*, 2022, **120**, 1–22.

115 W. Verweij and J.-P. Simonin, *J. Solution Chem.*, 2020, **49**, 1319–1327.

116 A. R. Crothers, C. J. Radke and J. M. Prausnitz, *Ind. Eng. Chem. Res.*, 2019, **58**, 18367–18377.

117 J. H. Hoff, *Études de dynamique chimique*, Frederik Muller & Company, 1884.

118 R. J. Lemire and M. W. Lister, *J. Solution Chem.*, 1976, **5**, 171–181.

119 S. Katayama, *J. Solution Chem.*, 1976, **5**, 241–248.

120 L. Onsager, *Trans. Faraday Soc.*, 1927, **23**, 341.

121 S. Naseri Boroujeni, B. Maribo-Mogensen, X. Liang and G. M. Kontogeorgis, *Fluid Phase Equilib.*, 2023, **567**, 113698.

This journal is © the Owner Societies 2025

Phys. Chem. Chem. Phys., 2025, **27**, 7703–7715 | 7715